GNC Design and Fuel Consumption Analysis in MMX Approach and Vertical Descent Phase

Yuki Matsumoto[1], Shinji Mitani[1], Go Ono[2], Naoki Okada[1], Yohsuke Takeo[1], Tatsuo Ueno[3], Yasuyuki Watanabe[4], Kentaro Watanabe[4], Tomohiro Yamaguchi[4], Daisuke Toyama[4]

(1) Japan Aerospace Exploration Agency, Tsukuba, Ibaraki, Japan
matsumoto.yuki@jaxa.jp, mitani.shinji@jaxa.jp, okada.naoki@jaxa.jp, takeo.yohsuke@jaxa.jp
(2) Japan Aerospace Exploration Agency, Sagamihara, Kanagawa, Japan
ono.go@jaxa.jp
(3) Mitsubishi Electric Software Corporation, Kamakura, Kanagawa, Japan
Ueno.Tatsuo@zs.MitsubishiElectric.co.jp
(4) Mitsubishi Electric Corporation, Kamakura, Kanagawa, Japan
Watanabe.Yasuyuki@dc.MitsubishiElectric.co.jp, Watanabe.Kentaro@eb.MitsubishiElectric.co.jp,
Yamaguchi.Tomohiro@ce.MitsubishiElectric.co.jp, Toyama.Daisuke@aj.MitsubishiElectric.co.jp

*Abstract –***Martian Moons eXploration (MMX) is a sample return mission from a Mars satellite (Phobos) currently planned in Japan. To achieve two landings with a limited amount of propellant, it is necessary to minimize propellant consumption in the design of the trajectory for the approach descent phase and in the design of the guidance and control law for the vertical descent phase. On the other hand, it is not enough to simply minimize the amount of propellant consumed because of mission-specific constraints, such as trajectory and attitude constraints imposed by the relative navigation sensor. Therefore, this paper proposes a design method for trajectory design and guidance control system design that minimizes propellant consumption under the mission-specific constraints of MMX. Simulations demonstrate the effectiveness of the proposed method.**

I. INTRODUCTION

Martian Moons eXploration（MMX）is a sample return mission from the Mars satellite Phobos [1]. The MMX mission is scheduled for launch in 2026, and the mission period is planned to be five years: one year for the outbound, three years for the stay, and one year for the return. During its stay, MMX is scheduled to make detailed observations of Phobos from a quasi-satellite trajectory (QSO) [2,3] and to make two descents and landings. In MMX, dozens of candidate landing target points will be selected after arrival at Phobos. Then, further detailed observations will be made to select a target landing point with an inclination of less than 10° and an undulation difference of less than 30 cm peak-to-peak. MMX requires a landing with an accuracy of ± 10 m relative to the target landing point, and a guidance accuracy of ±5 m is required considering the static settling after ground contact.

The guided descent sequence is divided into three phases: The Approach Descent Phase (ADP), the Vertical Descent Phase (VDP), and the free-fall phase. The ADP is the phase in which the spacecraft departs from the QSO and performs ballistic flight to an altitude of 2.2 km above the target point. In the VDP, the spacecraft is guided from an altitude of 2.2 km to an altitude of 10 m while absorbing the guidance errors accumulated in the ADP. In the final freefall phase, the thrusters are stopped to prevent soil contamination on the surface of Phobos, and the spacecraft will perform a freefall from an altitude of 10 m. In MMX, the amount of propellant consumed during the ADP and VDP must be reduced to achieve two descents with a limited amount of onboard propellant.

On the other hand, the spacecraft's attitude at ADP termination is constrained because the ADP requires the spacecraft to perform the VDP transition maneuver (VTM) at an attitude suitable for optical navigation to be performed in the VDP. In addition, since the plans for the VTM will be updated based on the Doppler results on the ground during the ADP, the ADP transition time must be set considering the Doppler calculation time and propagation delay from the Earth to Phobos. Furthermore, the guidance error at the end of the ADP affects the amount of propellant consumed by the VDP. Therefore, the guidance error must be suppressed at the end of the ADP. In the VDP, there are constraints on the measurement range of the altimeter used as a relative navigation sensor and the trajectory and attitude during descent for optical navigation.

Therefore, this paper proposes a design method for ADP reference trajectory and VDP guidance and control law that minimizes propellant consumption under MMX-specific constraints. In addition, since the amount of propellant consumed by the ADP varies with the latitude and longitude of the target landing point due to the characteristics of the QSO trajectory, the relationship between the latitude and longitude of the target landing point and the amount of propellant consumed is clarified through an exhaustive analysis.

II. PREREQUISITE

A. The guided descent sequence
The descent guidance sequence for MMX, which is the

---

premise of this study, is described in Fig. 1. In MMX, descent guidance is divided into three phases: The ADP, the VDP, and the freefall phase. As shown in Fig. 1, the policy is to absorb the errors accumulated in the ADP through the VDP. The following sections describe the details of the ADP and VDP sequences.
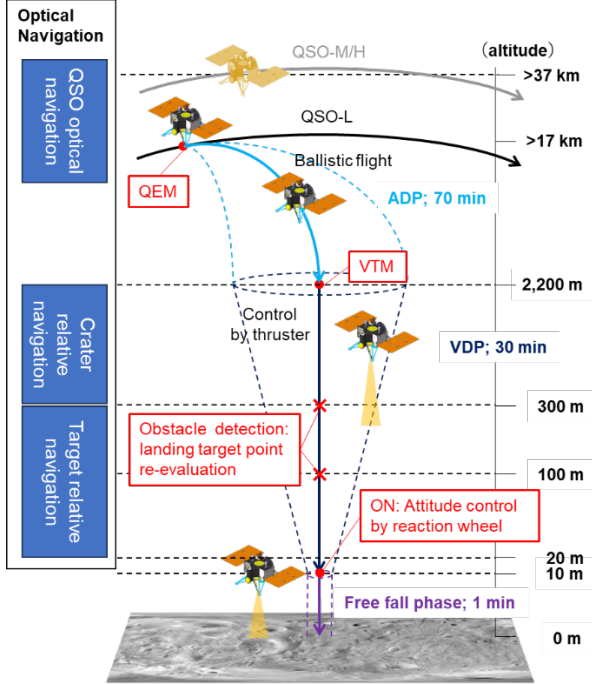
Fig. 1. Guided descent sequences

Approach Descent Phase
The ADP starts with a QSO Escape Maneuver (QEM), then performs a ballistic flight (unguided) to 2.2 km above the landing target, and finally performs a Vertical Transfer Maneuver (VTM). The two maneuver values are uploaded in advance via the ground operator. To suppress the expansion of navigation and guidance errors associated with the QEM, the Doppler scan is acquired for about 10 minutes after the QEM is completed, and the trajectory is calculated on the ground. After that, the VTM values are updated through ground planning systems using the updated trajectory determination values.

Vertical Descent Phase
In the VDP, the nominal descent start position and velocity after VTM, which is the I/F with ADP, are described as follows.

$$(\mathbf{r}_{\text{enu}}^{\text{T}}, \mathbf{v}_{\text{enu}}^{\text{T}}) \\ = (0\text{m}, 0\text{m}, 2200\text{m}, 0\text{m/s}, 0\text{m/s}, \text{-}1\text{m/s}) \quad (1)$$

Equation (1) is expressed in the ENU coordinate system: the origin of the ENU coordinate system is the landing target point, the E (East) axis is in the East direction

from the landing target point, the U (Up) axis is in the direction from the center of Phobos to the landing target point, and the N (North) axis is the outer product of the U and E axes.

In addition to the inertial sensor (IMU), the VDP will use an optical camera and altimeter to estimate the relative position and velocity on Phobos from an altitude of 2.2 km. During the VDP, terrain relative navigation using craters as features is implemented up to an altitude of 300 m. During this time, the spacecraft is oriented to the mean plane of the surface to increase the probability of success of optical navigation. Below an altitude of 300 m, the optical navigation switches to template matching in case there are no craters to be used as features. Since template matching prefers to use a feature-rich point as a template, at an altitude of 400 m, the spacecraft starts pointing to the best matching surface point, called the Virtual Target Point (VTP). At an altitude of 20m, it returns to the target point orientation for landing. Template matching requires that the VTP be pointed directly above the VTP to increase the success rate of optical navigation. Therefore, converging the horizontal error at an altitude of 400 m is necessary. In addition, due to the constraints of the spacecraft's communication antenna, a large rotation in the Yaw direction causes a risk that the antenna is not able to point to Earth; thus, rotation around the Yaw axis must be avoided during the descent. At 300 m and 100 m, an obstacle detection function is implemented. If an obstacle is identified around the current target point, the target point will be changed to ensure the safety of the spacecraft.

B. Accuracy requirement at ground contact
MMX requires a landing with 10 m accuracy. In addition, considering the residual velocity at ground contact, equipment failure, and spacecraft tipping over, the following I/F for ground contact is defined.

Table 1. Required accuracy at ground contact

Horizontal position error	± 5 m
Velocity error	Horizontal: ± 8 cm/s Vertical ：48 cm/s
Angle error	$\pm 5°$ (each axis)
Angular velocity error	$\pm 0.1°$/s (each axis)

III. DESIGN OF DESCENT SEQUENCE

A. Design of ADP reference trajectory
Since no guidance control is performed in the middle of the ADP, the design of the reference trajectory is crucial. In MMX, the Z-axis thrusters are mounted along the axis, but the X-axis and Y-axis thrusters are mounted inclined to the axis. QEM has enough time before the maneuver, so the maneuver can be performed after the spacecraft's

Z-axis is pointed in the maneuver direction. However, VTM must be performed at an attitude suitable for optical navigation (i.e., pointing toward the mean plane) to start optical navigation after completing the maneuver. Therefore, to keep the ΔV loss of VTM small, VTM must be performed only with thrusters in the spacecraft Z-axis direction at an attitude oriented to the mean plane, as shown in Fig. 2. In the ADP, the reference trajectory must be designed so that the total propellant consumption, including this canted loss, is small.
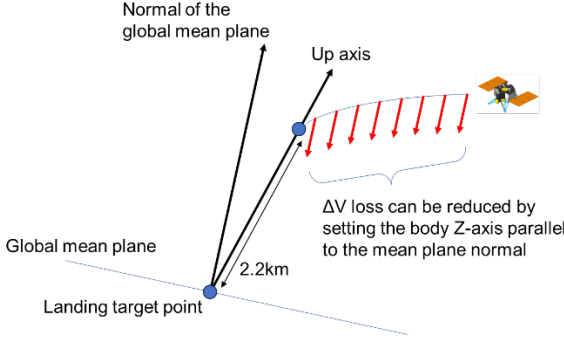
Fig. 2. Strategy to keep ΔV loss small

ΔV_{loss}, the loss ΔV generated by VTM, is calculated as follows: a control input of VTM, $\boldsymbol{u}_{\mathrm{VTM}}$ is assumed to be constant in the spacecraft fixed frame during the maneuver, and the following equation holds.

$$|\boldsymbol{u}_{\mathrm{VTM}}|_x \leq \boldsymbol{F}_{\max}|_x$$
$$|\boldsymbol{u}_{\mathrm{VTM}}|_y \leq \boldsymbol{F}_{\max}|_y \qquad (2)$$
$$|\boldsymbol{u}_{\mathrm{VTM}}|_z \leq \boldsymbol{F}_{\max}|_z$$

where $\boldsymbol{F}_{\max}$ is the maximum thrust vector in the spacecraft fixed frame. When $\boldsymbol{u}_{\mathrm{VTM}}$ is given, the ideal VTM ΔV ($\Delta \boldsymbol{V}_{\mathrm{VTM}}$) can be calculated using the spacecraft mass m and VTM execution time Δt_{VTM} as follows.

$$\Delta \boldsymbol{V}_{\mathrm{VTM}} = \frac{\boldsymbol{u}_{\mathrm{VTM}} \Delta t_{\mathrm{VTM}}}{m} \qquad (3)$$

To obtain the actual required ΔV, ΔV_{true} including the canted loss, the thruster assignment matrix is used to calculate the duty cycle of each thruster to achieve $\boldsymbol{u}_{\mathrm{VTM}}$. When the number of thrusters is M, ΔV_{true} can be described as follows.

$$\Delta V_{\mathrm{true}} = \sum_{i=1}^{M} d_i \cdot F_{\mathrm{thrust}} \cdot \Delta t_{\mathrm{VTM}} / m \qquad (4)$$

F_{thrust} is the magnitude of thruster force. From the above, ΔV_{loss} is defined as follows.

$$\Delta V_{\mathrm{loss}} = \Delta V_{\mathrm{true}} - \|\Delta \boldsymbol{V}_{\mathrm{VTM}}\| \qquad (5)$$

Therefore, ADP defines the following objective function J to design the optimal reference trajectory.

$$J = \min(\|\Delta \boldsymbol{V}_{\mathrm{QEM}}\| + \|\Delta \boldsymbol{V}_{\mathrm{VTM}}\| + \Delta V_{\mathrm{loss}}) \qquad (6)$$

Where, $\Delta \boldsymbol{V}_{\mathrm{QEM}}$ is ΔV of QEM.

In the ADP, guidance control is not performed according to the reference trajectory. Therefore, at the end of the ADP, guidance errors are generated due to trajectory control errors, trajectory determination errors, and gravity estimation errors. MMX plans to absorb this guidance error with the VDP, but a large guidance error is undesirable because it causes an increase in the onboard crater map size and the amount of propellant consumed to absorb the guidance error. Therefore, when designing the ADP reference trajectory, evaluating the ADP termination guidance error by Monte Carlo simulation is necessary as well.

B. VDP Consumed Propellant Minimum Trajectory Design

To design the VDP guidance and control law, we first perform the minimum consumption propellant trajectory design based on [4] for the case without MMX-specific constraints. Based on the discretized CR3BP equation of motion, dividing the trajectory into N segments, and assuming a constant input vector for each segment, the ΔV optimization problem is formulated as shown in Table 2.

Table 2. Optimization problem setting

Parameters	Values	Complement
Design variables	$\boldsymbol{u}_i \ (i = 1 \cdots N)$	Control input 3-component for each segment
Constraints	$\boldsymbol{x}_{\mathrm{ini}} = (0,0,2200,0,0,-1)^{\mathrm{T}}$	ENU frame ([m], [m/s])
	$\boldsymbol{x}_{\mathrm{end}} = (0,0,10,0,0,0)^{\mathrm{T}}$	ENU frame ([m], [m/s])
Objective function	$J = \min \sum_{i=1}^{N} \|\boldsymbol{u}_i\|$	
Number of orbit segments	100	
VDP transition time	1,800 s	Fixed to 1,800 s

Fig. 3 shows the results of the minimum consumption propellant trajectory design in this problem setting.
As shown in Fig. 3, ΔV hardly increases during the period from about 300 seconds to 1400 seconds, indicating that the spacecraft is almost uncontrolled during this period. In other words, providing control

acceleration at the beginning and end of the profile and minimizing orbit control in the middle of the profile lead to a reduction in the amount of propellant consumed. Based on these results, we examine the VDP guidance and control law.
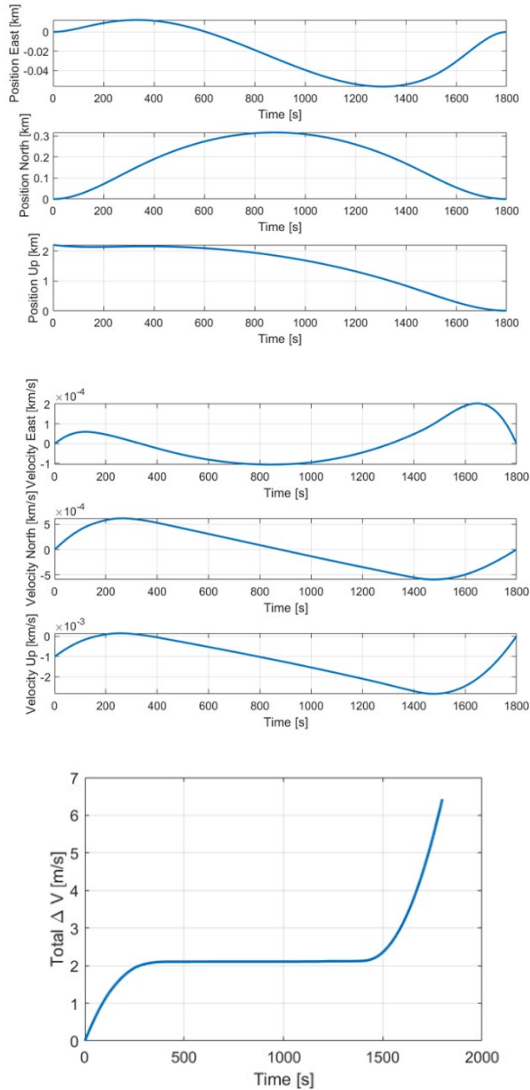
Fig. 3. Position, velocity, and ΔV transitions

C. Design of VDP guidance and control law

A VDP guidance and control law has been designed based on the results of the previous section. The VDP is a phase to absorb the error accumulated in the ADP and guide the robot to the freefall starting position. Based on the assumptions made in the previous chapter, Table 3 shows the constraints that must be satisfied in the VDP.

Table 3. Constraints

c-1	The descent starts at an altitude of 2.2 km, and the horizontal guidance error assumed at the end of the ADP is to be converged by an altitude of 400 m.
c-2	The spacecraft is oriented in the direction of the mean plane from 2.2 km to 400 m, in the direction of the VTP from 400 m to 20 m, and in the direction of the landing target point from 20 m to 0 m (Large rotations around the Yaw direction during descent should be avoided).
c-3	The spacecraft satisfies the required accuracy at ground contact even in the case of thrust error.

To compensate for position and velocity errors caused by thruster variation and individual output variation, the VDP guidance control law uses feedback (FB) control based on the amount of deviation between the current position and velocity and the target position and velocity and feedforward (FF) control to compensate for gravity acceleration at the target landing point. This guidance control law further divides guidance into two phases during VDP (Fig. 4).

- Phase 1: Phase to converge the horizontal position error
- Phase 2: Phase to accelerate to the horizontal velocity at the start of freefall

When the estimated altitude reaches the intermediate guidance target altitude, the system transitions from Phase 1 to Phase 2. When the estimated altitude reaches the freefall starting altitude, the system transitions from Phase 2 to the freefall phase.
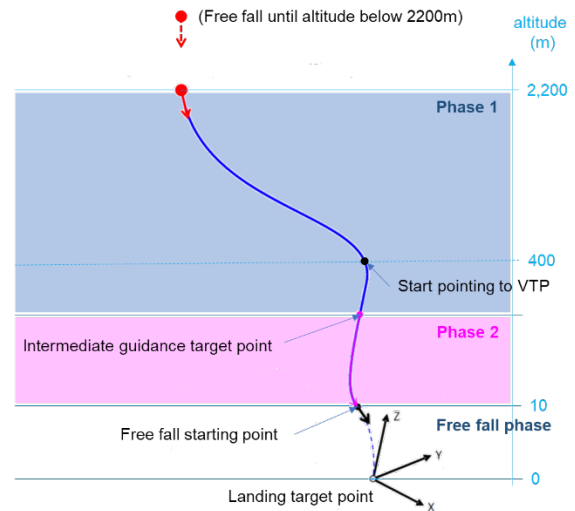
Fig. 4. VDP guidance control profile

With FB control, the acceleration a_{thr} that can be reliably output for orbit control is set. As shown in constraint c-2 defined in Table 3, the thruster duty cycle is allocated not only for orbit control but also for attitude control so that the desired attitude control can be performed because the direction of pointing changes

during the VDP. To satisfy constraint c-1, the tracking velocity $V_{\mathrm{cnst}}[\mathrm{m/s}]$ is set based on a_{thr} and the ADP terminal guidance error. By setting the tracking velocity, the profile absorbs the error at a constant speed; thus, the profile is close to uncontrolled after the tracking velocity is reached. This is similar to the result of the minimum propellant consumption trajectory design described in the previous section and leads to suppressing propellant consumption.

The vertical tracking velocity is set onboard so that the horizontal error can be converged by 400 m altitude at which the attitude pointing for optical navigation occurs. In the minimum propellant consumption trajectory design described in the previous section, propellant consumption was suppressed by making the middle of the profile freefall. Therefore, after the horizontal position error converges, the vertical position and velocity control is stopped temporarily, and the design is made to accelerate by gravity. After that, position and velocity control in the Z direction is resumed when the distance required to decelerate to the velocity at the start of freefall is reached.

The end position and velocity of Phase 1 and Phase 2 are determined as follows: the end position and velocity of Phase 2 is defined as the acceleration of gravity on Phobos $G_{\mathrm{p}}[\mathrm{m/s^2}]$, the altitude at the start of freefall $h_{\mathrm{ff}}[\mathrm{m}]$, and the vertical velocity $v_{\mathrm{ff}}[\mathrm{m/s}]$. Assuming that G_{p} is constant during free fall, the time taken for freefall (freefall time) $t_{\mathrm{ff}}[\mathrm{s}]$ is as follows.

$$t_{\mathrm{ff}} = \frac{\left(-v_{\mathrm{ff}} - \sqrt{v_{\mathrm{ff}}^2 - 2G_{\mathrm{p}}|_z h_{\mathrm{ff}}}\right)}{G_{\mathrm{p}}|_z} \tag{7}$$

From t_{ff}, the Phase 2 end position $P_{\mathrm{ff}}[\mathrm{m/s}]$ and velocity $V_{\mathrm{ff}}[\mathrm{m/s}]$ are as follows.

$$P_{\mathrm{ff}} = \begin{pmatrix} 0.5G_{\mathrm{p}}|_x t_{\mathrm{ff}}^2 \\ 0.5G_{\mathrm{p}}|_y t_{\mathrm{ff}}^2 \\ h_{\mathrm{ff}} \end{pmatrix}, V_{\mathrm{ff}} = \begin{pmatrix} -G_{\mathrm{p}}|_x t_{\mathrm{ff}} \\ -G_{\mathrm{p}}|_y t_{\mathrm{ff}} \\ v_{\mathrm{ff}} \end{pmatrix} \tag{8}$$

Next, the Phase 1 end position and velocity are determined. In Phase 2, to output the desired force and ensure that the freefall start point's horizontal position and v are reached, the time t_{phase2} of Phase 2 is twice the freefall time. In addition, the horizontal direction is set to accelerate at half the acceleration of gravity, and the vertical direction is given the acceleration $a_{\mathrm{thr}}|_z$ that can be generated. In other words, the time t_{phase2} and acceleration a_{phase2} of Phase 2 are as follows.

$$t_{\mathrm{phase2}} = 2t_{\mathrm{ff}} \tag{9}$$

$$a_{\mathrm{phase2}} = \begin{pmatrix} -0.5G_{\mathrm{p}}|_x \\ -0.5G_{\mathrm{p}}|_y \\ a_{\mathrm{thr}}|_z \end{pmatrix} \tag{10}$$

In order to perform uniformly accelerated motion with constant acceleration in (10) for the time in (9) and to reach the target state in (8), the end position $P_{\mathrm{wp}}[\mathrm{m/s}]$ and end velocity $V_{\mathrm{wp}}[\mathrm{m/s}]$ of Phase 1 are the following.

$$P_{\mathrm{wp}} = \begin{pmatrix} -\dfrac{a_{\mathrm{phase2}}|_x t_{\mathrm{phase2}}^2}{2} + P_{\mathrm{ff}}|_x \\ -\dfrac{a_{\mathrm{phase2}}|_y t_{\mathrm{phase2}}^2}{2} + P_{\mathrm{ff}}|_y \\ \dfrac{a_{\mathrm{phase2}}|_z t_{\mathrm{phase2}}^2}{2} - v_{\mathrm{ff}} t_{\mathrm{phase2}} + h_{\mathrm{ff}} \end{pmatrix} \tag{11}$$

$$V_{\mathrm{wp}} = \begin{pmatrix} 0 \\ 0 \\ v_{\mathrm{ff}} - a_{\mathrm{thr}}|_z t_{\mathrm{phase2}} \end{pmatrix}$$

IV. NUMERICAL SIMULATION

In this chapter, the design validity of a series of descent sequences with reduced propellant consumption is demonstrated by numerical simulations.

A. ADP trajectory analysis
In this section, the evaluation is performed for the landing target points shown in Table 4.

Table 4. Latitude and longitude of landing target point

latitude / longitude [deg]	25.8 / -164.6

The ADP transition time is set to 70 min to account for the Doppler analysis on the ground, and the ΔV and ADP termination error are evaluated when the QEM start phase angle θ is changed. The definition of θ is shown in Fig. 5.
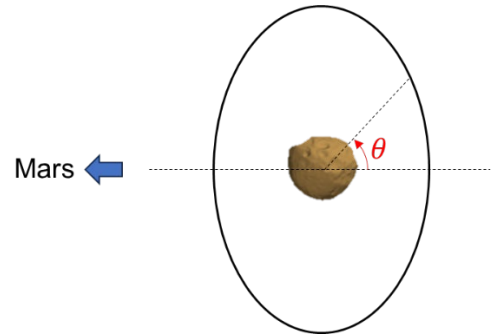
Fig. 5. The definition of θ

Table 5 shows the optimization problem settings, and Table 6 shows the analysis conditions. The ADP termination guidance error is evaluated by a 1000-particle Monte Carlo simulation based on the QSO orbit determination accuracy, control error, and GM error. The orbit determination accuracy is an intermediate value among the values assumed for MMX.

Table 5. Optimization problem setting

	Values
Design variables	$\boldsymbol{u}_{\mathrm{QEM}}^{\mathrm{BODY}}$ (constant)
	$\boldsymbol{u}_{\mathrm{VTM}}^{\mathrm{BODY}}$ (constant)
	Δt_{QEM}
	Δt_{VTM}
Constraints	θ : θ varies from 0° to 90° in 5° increments
	ADP transition time: 70 min
	Position and velocity after VTM $(r_{\mathrm{e}}, r_{\mathrm{n}}, r_{\mathrm{u}}) = (0,0,2.2)$ [km] $(v_{\mathrm{e}}, v_{\mathrm{n}}, v_{\mathrm{u}}) = (0,0,-1.0)$[m/s]
Objective function	Equation (6)

Table 6. Analysis condition

	values
Phobos shape model	Willner model [5]
Dynamics model	CR3BP
m	1929.4 [kg]
$\boldsymbol{F}_{\max}$	$(36.4,\ 17.0,\ 40.2)^{\mathrm{T}}$[N]
F_{thrust}	20.1 [N]
Monte-Carlo simulation	
Number of particles	1,000 times per each target point
Orbit determination accuracy	30 km QSO $(r_{\mathrm{r}}, r_{\mathrm{t}}, r_{\mathrm{n}}) = (40, 93, 4)$[m] (1σ) $(v_{\mathrm{r}}, v_{\mathrm{t}}, v_{\mathrm{n}}) = (30, 14, 1)$[mm/s] (1σ)
Control error	Magnitude: 5% (3σ) Direction: 1° (3σ)
GM error	1.5% (3σ)

The results of the analysis are shown in Fig. 6. As can be seen from Fig. 6, the loss ΔV and total ΔV are minimum at $\theta = 10°$. On the other hand, the ADP termination error in the East direction becomes smaller as θ increases, while the error in the Up direction becomes significantly smaller when θ exceeds 40°.
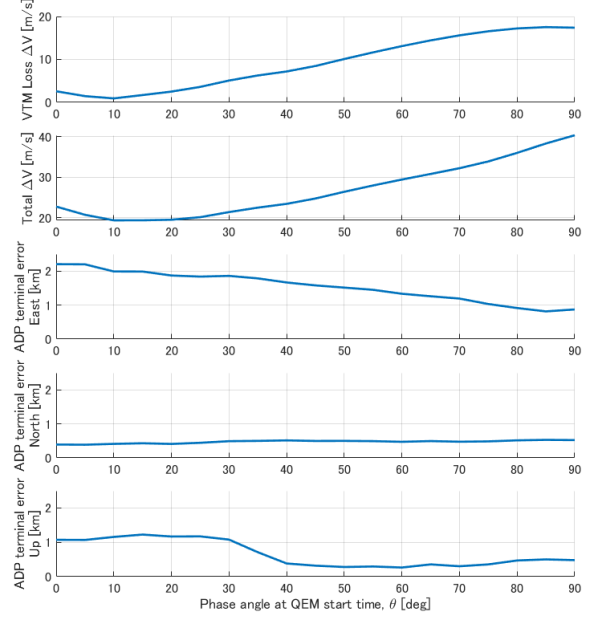
Fig. 6. ΔV and ADP termination error when varying θ

As seen from Fig. 6, the loss ΔV and total ΔV are minimum at $\theta = 10°$. On the other hand, the ADP termination error in the East direction becomes smaller as θ increases, while the error in the Up direction becomes significantly smaller when θ exceeds 40°. Here, the trajectory at $\theta = 40°$ is used as the ADP reference trajectory, as both ΔV and ADP termination error are small. The results of the Monte Carlo simulation at $\theta = 40°$ are shown in Fig. 7 and Table 7.
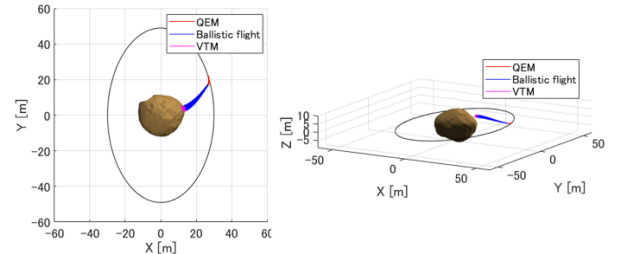
Fig. 7. Monte Carlo simulation at $\boldsymbol{\theta = 40°}$

Table 7. ADP termination guidance error at $\theta = 40°$

(East, North, Up)	(1.67, 0.49, 0.40) [km] (3σ)

B. VDP Monte-Carlo simulation
In this section, Monte Carlo simulations are performed for the ADP termination error obtained in the previous section. A Monte Carlo simulation of 100 particles is performed. The simulation conditions are shown in Table 8. The simulation results are shown in Table 9 and Fig. 8. As shown in Fig. 8 (a), the horizontal error converges by an altitude of 400 m, indicating that the constraint c-1 in Table 3 is satisfied. In Fig. 8 (c), the roll angle is offset by about 20° until the halfway point

because the particles are oriented in the mean plane direction, thus satisfying constraint c-2 for all particles. Furthermore, as shown in Table 9, the ground I/F is also satisfied, so constraint c-3 is also satisfied. Thus, the proposed method numerically satisfies the constraints of MMX.

Table 8. Monte Carlo simulation condition

Parameter		Value	Complement
VDP guidance control law	h_{ff}	10 m	
	v_{ff}	-10 cm/s	
	$\boldsymbol{a}_{\text{thr}}$	$(0.0045, 0.0035, 0.0065)^{\text{T}}$ m/s²	
	$\boldsymbol{V}_{\text{cnst}}$	$(1.1, 0.7, 0.8)^{\text{T}}$ m/s	
	t_{phase2}	$2t_{\text{ff}}$	
Thruster model	Force	Uniform 90% for 20.1N	
Phobos model	Gravity model	Phobos: Polyhedron model [6] Mars: point-mass model	Gravity estimation error is 20%.
	Shape model	Willner model [5]	

Table 9. Monte Carlo simulation results summary

		States of the spacecraft at ground contact				Total ΔV [m/s]
		Position [m]	Velocity [cm/s]	Angle [°]	Angular velocity [°/s]	
mean	E	-0.0908	-0.8416	0.0059	0.0059	19.38
	N	-1.5418	-3.7721	-0.0022	-0.0022	
	U	-0.0094	-31.5859	0.0054	0.0054	
3σ	E	0.7466	1.3039	0.0191	0.0191	5.26
	N	0.8434	1.1016	0.0127	0.0127	
	U	0.0180	0.2312	0.0211	0.0211	
Required accuracy at ground contact		Horizontal: ±5	Horizontal: 8 Vertical: -48	±5 (each axis)	±0.1 (each axis)	

(a) E-U, N-U position (ENU frame)

(b) E-U, N-U position (ENU frame) magnification

(c) Angle (ENU frame)

(d) Angular velocity (ENU frame)
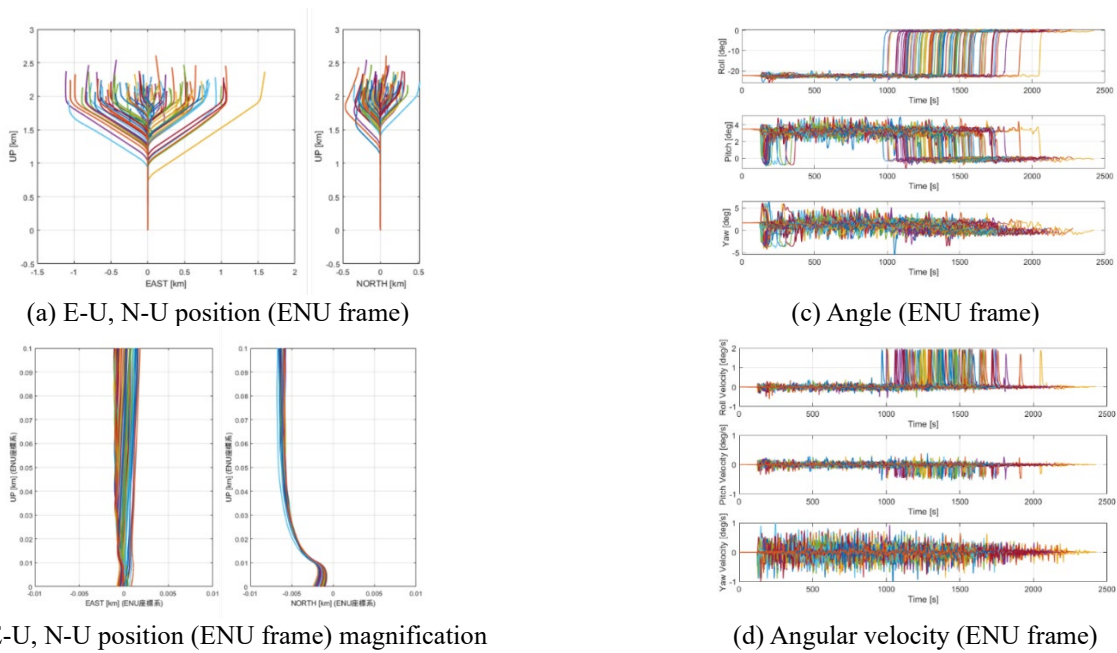
Fig. 8. Descent orbit and time response of angle and angular velocity

C. Evaluation of Propellant Consumption for landing site

Due to the characteristics of the QSO orbit, the amount of propellant required for ADP varies depending on the landing target point. Therefore, we evaluate the ΔV required for each landing target point. In this section, two cases are evaluated: one in which the ADP transition time is fixed at 70 min and the other in which the ADP transition time is not restricted. The evaluation points are shown in Table 10. The optimization problem settings are the same as in Table 5 except for the ADP transition time, and the analysis conditions are the same as in Table 6.

Table 10. Latitude and longitude of landing target point

Latitude	-30° to 30° in 10° increments
Longitude	-180° to 180° in 10° increments

The results of evaluating ΔV at each landing site are shown in Fig. 9 and Fig. 10. As can be seen from these figures, the total ΔV is smaller for all landing sites when the ADP transition time is not constrained. It can also be seen that the longitude ranges of -60°~0° and 120°~180° are regions where ΔV is relatively small in both cases.
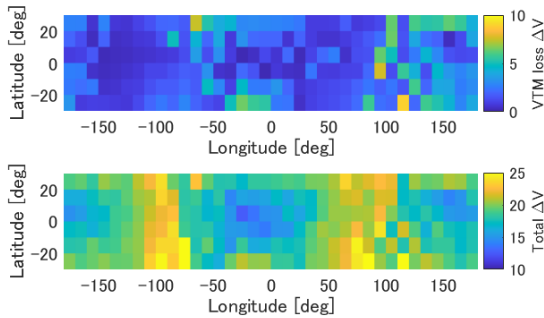
Fig. 9. ΔV (ADP transition time fixed to 70 min)
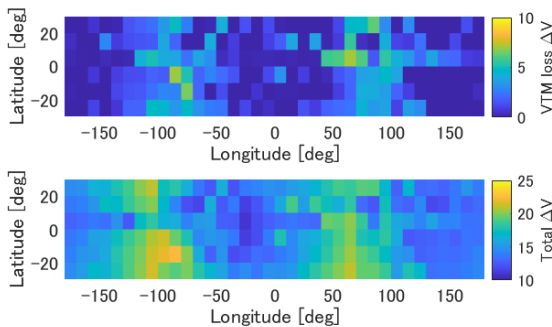
Fig. 10. ΔV (no ADP transition time constraint)

From the above, it can be seen that for a profile descending from a QSO as in MMX, there is a range of target point latitude and longitude that is favorable for landing in terms of the amount of propellant consumed. MMX is designed to descend anywhere within ±30 degrees latitude because the landing target point will be determined after arrival at Phobos. However, if some unexpected event occurs during actual operations, such as a lower-than-expected amount of remaining propellant, the results of this analysis could be used as material for selecting a landing site.

V. CONCLUSION

A design method for ADP reference trajectory and VDP guidance and control law with reduced propellant consumption under the constraints specific to MMX was proposed. The relationship between the latitude and longitude of the target landing point and the amount of propellant consumed was also clarified through an exhaustive analysis since the amount of propellant consumed by ADP varies with the latitude and longitude of the target landing point due to the characteristics of the QSO trajectory. As the terminal guidance error produced by ADP affects the ΔV of VDP, it is essentially necessary to optimize ΔV as a whole descent without separating ADP and VDP. In the future, a framework for overall optimization will be developed.

REFERENCES

[1] Kawakatsu, Y., Kuramoto, K., Usui, T., Sugahara, H., Ootake, H., Yasumitsu, R., Yoshikawa, K., Mary, S., Grebenstein, M., Sawada, H., Imada, T., Shimada, T., Ogawa, K., Otsuki, M., Baba, M., Fujita, K., Zacny, K., van Dyne, D., Satoh, Y., and Tokaji, A.: Preliminary Design of Martian Moons eXploration (MMX). *Acta Astronautica*, 2023, 202: 715-728.

[2] Pushparaj, N., Baresi, N., and Kawakatsu, Y.: Design of transfer trajectories between planar and spatial quasi-satellite orbits. AIAA Scitech 2020 Forum, 2020. p. 2179.

[3] Pushparaj, N., Baresi, N., and Kawakatsu, Y.: Martian Moons eXploration transfer analysis between planar and spatial QSOs around Phobos. International Astronautical Congress, 2021.

[4] Kayama, Y., Bando, M., Hokamoto, S.: Minimum fuel trajectory design using sparse optimal control in three-body problem, AIAA Scitech 2020 Forum, 2020.

[5] Willner, K., Shi, X., and Oberst, J.: Phobos' shape and topography models. *Planetary and Space Science*, 2014, 102, 51-59.

[6] Werner, R. A., and Scheeres, D. J.: Exterior gravitation of a polyhedron derived and compared with harmonic and mas-con gravitation representations of asteroid 4769 Castalia. *Celestial Mechanics and Dynamical Astronomy*, 1996, 65, 313-344.